Edge current density and pressure profile evolution during nitrogen seeded improved H-mode scenarios on ASDEX Upgrade

M.G. Dunne[1], E. Wolfrum[1], A. Burckhart[1], R. Fischer[1], L. Giannone[1], P.J. McCarthy[2], E. Viezzer[1], the ASDEX Upgrade Team[1]

[1] *Max-Planck-Institut für Plasmaphysik, D-85748 Garching,Germany*

[2] *Department of Physics, University College Cork, Cork, Ireland*

Operation in the metal walled machines ASDEX Upgrade (AUG) and JET typically requires the use of a deuterium gas puff. Consequently, confinement degradation due to the resulting higher density has been observed on both machines in comparison to operation with a carbon wall[1, 2]. However, when extrinsic seeding of low-Z impurities is applied on AUG, JET and also Alcator C-Mod[3], the confinement improves to levels seen with carbon wall operation.

This confinement improvement is observed to originate in the pedestal at both AUG and JET, which implies changes in the pedestal structure and stability with increased Z_{eff}. In this contribution, we present the pedestal structure, its impact on the edge current density, and test the peeling-balooning stability of AUG discharge #29254 in which the confinement improved by 40% with nitrogen seeding[4]. This discharge contained a short reference phase, followed by a nitrogen seeded phase and featured a β_N increase from 1.8-2.2.

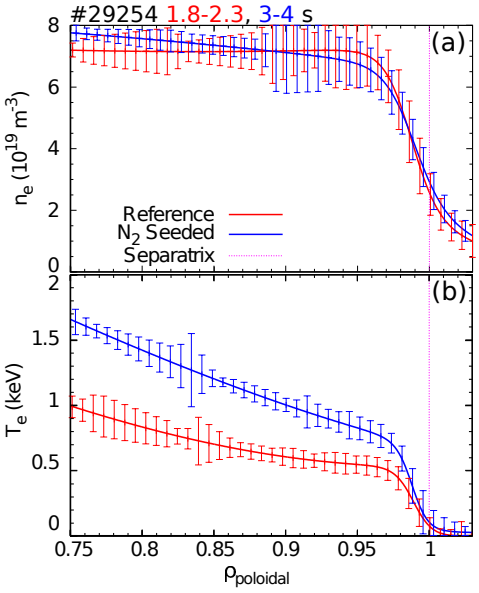

Figure 1: (a) electron density and (b) electron temperature profiles for reference (red) and seeded (blue) timepoints during discharge #29254 showing the steeper and higher electron temperature pedestal in response to nitrogen seeding.

Figure 1 shows (a) the electron density and (b) the electron temperature profiles for the reference phase (red profiles) and nitrogen seeded phase (blue profiles). All data are ELM-synchronised and taken during the time window between 3.5 and 0.5 ms before an ELM crash. The error bars indicate the 1σ scatter of the raw data from the respective diagnostics.

From this figure it is clear that the confinement improvement comes from the electron temperature pedestal. While the density pedestal is almost unchanged in the nitrogen seeded phase, both the gradient and height of the temperature pedestal increase. This increase propagates into the core plasma via stiff profiles, thus delivering the large confinement increase. Ion temperatures are not shown here, though the behaviour is similar to that of the electron temperature.

These profiles were taken as input for the CLISTE equilibrium code[5] in order to analyse the edge current density[6]. Magnetic data from 45 poloidal field probes and flux loop difference measurements

(taken throughout the discharge at a sampling rate of 10 kHz) were taken during the same intervals as the kinetic data. Measurements of the scrape-off layer current were also included to further constrain the equilibrium solution. Figure 2 shows the reconstructed (a) local toroidal and (b) flux surface averaged parallel current densities for both timepoints, with the same colour coding as above. Additionally, figure 2(b) shows the neoclassically calculated edge current density profiles (dashed lines and boxes) for both timepoints, using the equations provided in Sauter et al.[7, 8] for bootstrap and Ohmic current drives.

The local current density peak is increased during the seeded phase; this is due to the increased pressure gradient seen in figure 1 through both the Pfirsch-Schlüter drive and, one could expect, through an increased bootstrap drive. However, when examining the flux surface averaged current density, the latter appears not to be the case. It is clear from both the CLISTE results (solid lines) and neoclassical calculations (dashed lines) that the bootstrap current does not change between the two phases. This can be understood by considering the inputs for the calculated bootstrap current; the temperature and density profiles and the effective charge profile. In the cases presented here, the reference phase has a Z_{eff} of 1.3 at the pedestal top which increases to 1.9 during the nitrogen seeded phase. This increases the collisionality, lowering the efficiency of the bootstrap drive and thus compensating the increased drive from the steeper electron temperature profile.

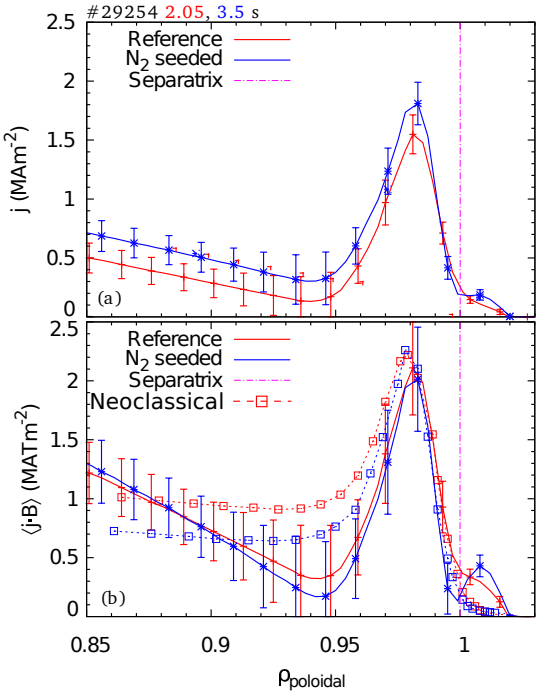

Figure 2: (a) local LFS midplane current density with 1σ confidence bands from CLISTE. (b) flux surface averaged current density from CLISTE (solid) and neoclassical calculations (dashed). While the local current density increases, the flux surface average remains the same.

This exact phenomenology is not always the case, however. While in this case the temperature gradient increase exactly compensates the lower bootstrap efficiency due to increased Z_{eff}, cases also exist where the current density decreases, or increases. Examples of these cases are shown in figure 3 for discharge pair #24681/2, where the current density decreased as the confinement increased, and for discharge #29874, which featured a similar confinement increase as #29254, but an overall increase in the current density. Plotted in figure 3 are the current densities resulting from CLISTE (stars) for reference (red) and nitrogen seeded (blue) cases. These are then compared to the neoclasssical current density using the Z_{eff} profiles interpreted using a Bayesian analysis of line integrated Bremsstrahlung measurements[9] (boxes).

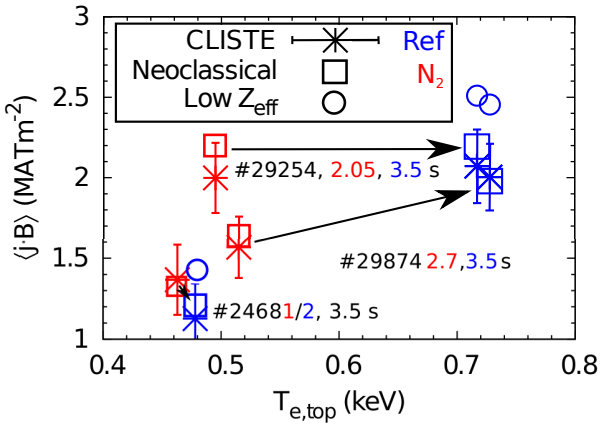

Figure 3: Flux surface averaged current density from CLISTE (stars) compared with neoclassical calculations (boxes) using the interpreted Z_{eff} profiles. Also shown are the calculated current densities assuming the unseeded Z_{eff} values.

Shown for comparison in the nitrogen seeded cases are the calculated current density if Z_{eff} had remained unchanged, but with the improved temperature profiles (circles); as expected, this demonstrates that the increased Z_{eff} value serves to decrease the flux surface averaged currrent density. This combination of an increased local current density at the LFS, which stabilises ballooning modes, and decreased flux surface averaged current density which stabilises the peeling mode could be the cause of increased confinement observed when low-Z impurities are seeded.

To test this hypothesis, the ideal MHD stability chain which has been implemented at AUG (see [10]) was used to analyse the pedestal stability for discharge #29254. The workflow of this chain is as follows: the experimental data are first used as constraints in the interpretive equilibrium code CLISTE, where the pressure gradient and current density are determined self-consistently. This equilibrium is then refined in two steps, first using the predictive version of CLISTE, and then using the fixed boundary equilibrium solver HELENA. Once the equilibrium has been created by HELENA, it is used as the basis for the j-α routine[11], which, in the cases shown here, varies the height of the pedestal at a fixed width, and the height of the edge current density peak while keeping the plasma beta and total current constant. This creates a grid of equilibrium solutions which are then evaluated using the ILSA code[11]. This analysis has been done for the two timepoints shown in this paper, the results of which are shown in figure 4.

Both figures have the same axis range, with the stars indicating the operational points. The stability boundary is determined as $\gamma_{crit}\tau_{Alfven} = 0.06$, where γ_{crit} is the growth rate of the most unstable toroidal mode number as calculated by ILSA. This is a somewhat arbitrary criterion, but in a range of stability analyses it clearly delineates the region in stability space with no unstable modes from that where clearly unstable modes are found. The analysis of these two cases shows an interesting conclusion; the stability boundary in the seeded case shifts towards higher pressure gradients, allowing the reference point to shift along with it. While the agreement between the operational points and the boundary is not perfect, a discrepancy of the boundary location and operational point of 15% is within acceptable levels of uncertainty. More important is the observed trend. The increased beta in the seeded case allows a higher pedestal pressure gradient to be sustained before an ELM occurs, thus facilitating higher confinement.

Given the hypothesis that pedestal structure changes create the improved confinement, this argument may seem somewhat circular. However, it points to a mechanism allowing confinement improvement; some initial mechanism increases the confinement by a small amount, which shifts the operational point to a higher pressure gradient and pedestal height. This pedestal height increase then propagates into the core plasma via stiff profiles and thus increases the stored energy.

The higher plasma beta then further stabilises the edge plasma, allowing yet higher pressure gradients to be attained, which can propagate into the core plasma until a new equilibrium position is reached. This initial seed mechanism could be related to the current density; if the current density is initially suppressed by increasing Z_{eff}, the operational point first moves downwards in stability space. If the stability boundary shape in figure 4 is accurate, then this downward movement would also be accompanied by a shift to higher pressure gradients. If the mechanism setting the height and width of the density pedestal is unaffected by this change, then the temperature gradient can increase, leading to the situation analysed here.

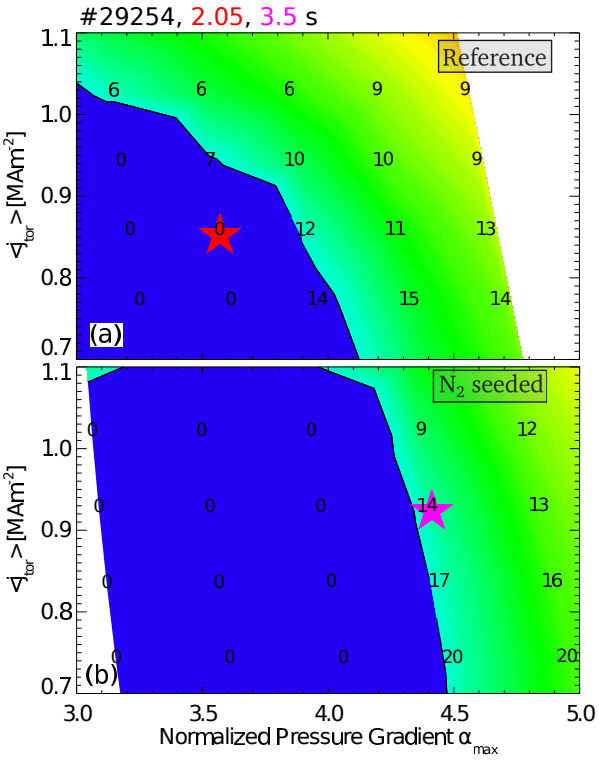

Figure 4: Stability diagrams for (a) the reference timepoint and (b) the nitrogen seeded timepoint. Both the stability boundary and the operational point shift towards higher pressure gradients with impurity seeding.

This mechanism depends strongly on the shape of the stability boundary. For example, if the stability boundary is steeper, then the effect on confinement will be smaller for the same increase in Z_{eff}. If this is extended further and the slope of the ballooning side of the stability boundary becomes positive, then the confinement would decrease with increased impurity seeding. Since extrinsic impurity seeding is a requirement for power exhaust in future fusion reactors, modelling of the pedestal structure and its response to impurity seeding is of great importance to judge its impact on the predicted plasma performance in such devices.

References

[1] J. Schweinzer, et al. *NF*, 51(11), 2011.

[2] M.N.A. Beurskens, et al. *PPCF*, 55(12), 2013.

[3] M.L. Reinke, et al. *JNM*, 415(1), 2011.

[4] A. Kallenbach, et al. *PPCF*, 55(12), 2013.

[5] P.J. McCarthy. *PoP*, 6(9), 1999.

[6] M.G. Dunne, et al. *NF*, 52(12), 2012.

[7] O. Sauter, et al. *PoP*, 6(7), 1999.

[8] O. Sauter, et al. *PoP*, 9(12), 2002.

[9] S.K. Rathgeber, et al. *PPCF*, 52(9), 2010.

[10] A. Burckhart. PhD thesis, LMU, 2013.

[11] C. Konz, et al. In *EPS, Strasbourg*, 2011.